














RESEARCH ARTICLE

Interictal high-frequency oscillations, spikes, and connectivity profiles: A fingerprint of epileptogenic brain pathologies

Barbora Sklenarova^{1,2}  | Eva Zatloukalova^{1,2}  | Jan Cimbalnik²  |
 Petr Klimes^{2,3}  | Irena Dolezalova^{1,2}  | Martin Pail^{1,2,3}  | Jitka Kocvarova¹  |
 Michal Hendrych⁴  | Marketa Hermanova⁴  | Jean Gotman⁵  |
 François Dubeau⁵ | Jeffery Hall⁵ | Raluca Pana⁵  | Birgit Frauscher⁵  |
 Milan Brazdil^{1,6} 

¹Brno Epilepsy Center, Department of Neurology, St. Anne's University Hospital and Medical Faculty of Masaryk University, Brno, Czech Republic

²International Clinical Research Center, St. Anne's University Hospital and Medical Faculty of Masaryk University, Brno, Czech Republic

³Institute of Scientific Instruments of the Czech Academy of Sciences, Brno, Czech Republic

⁴First Department of Pathology, St. Anne's University Hospital and Faculty of Medicine, Masaryk University, Brno, Czech Republic

⁵Montreal Neurological Institute and Hospital, McGill University, Montreal, Quebec, Canada

⁶Behavioral and Social Neuroscience Research Group, Central European Institute of Technology, Masaryk University, Brno, Czech Republic

Correspondence

Eva Zatloukalova, Brno Epilepsy Center, Department of Neurology, St. Anne's University Hospital and Medical Faculty of Masaryk University, Brno, Czech Republic.
 Email: eva.zatloukalova@fnusa.cz

Funding information

Fonds de Recherche du Québec - Santé 2021-2025, Grant/Award Number: Chercheur-boursier clinicien Senior; Agentura Pro Zdravotnický Výzkum České Republiky, Grant/Award Number: NU22-08-00278 and NU22-04-00366; Canadian Institutes of Health Research, Grant/Award Number: PJT-175056; George E. Hewitt Foundation for Medical Research; Grantová Agentura České Republiky, Grant/Award Number: 22-28784S

Abstract

Objective: Focal cortical dysplasia (FCD), hippocampal sclerosis (HS), nonspecific gliosis (NG), and normal tissue (NT) comprise the majority of histopathological results of surgically treated drug-resistant epilepsy patients. Epileptic spikes, high-frequency oscillations (HFOs), and connectivity measures are valuable biomarkers of epileptogenicity. The question remains whether they could also be utilized for preresective differentiation of the underlying brain pathology. This study explored spikes and HFOs together with functional connectivity in various epileptogenic pathologies.

Methods: Interictal awake stereoelectroencephalographic recordings of 33 patients with focal drug-resistant epilepsy with seizure-free postoperative outcomes were analyzed (15 FCD, 8 HS, 6 NT, and 4 NG). Interictal spikes and HFOs were automatically identified in the channels contained in the overlap of seizure onset zone and resected tissue. Functional connectivity measures (relative entropy,

Barbora Sklenarova, Eva Zatloukalova, Irena Dolezalova, Martin Pail, Jitka Kocvarova, and Milan Brazdil are members of the European Reference Network EpiCARE.

Barbora Sklenarova and Eva Zatloukalova contributed equally and share first authorship.

This is an open access article under the terms of the [Creative Commons Attribution-NonCommercial-NoDerivs](https://creativecommons.org/licenses/by-nc-nd/4.0/) License, which permits use and distribution in any medium, provided the original work is properly cited, the use is non-commercial and no modifications or adaptations are made.

© 2023 The Authors. *Epilepsia* published by Wiley Periodicals LLC on behalf of International League Against Epilepsy.

linear correlation, cross-correlation, and phase consistency) were computed for neighboring electrode pairs.

Results: Statistically significant differences were found between the individual pathologies in HFO rates, spikes, and their characteristics, together with functional connectivity measures, with the highest values in the case of HS and NG/NT. A model to predict brain pathology based on all interictal measures achieved up to 84.0% prediction accuracy.

Significance: The electrophysiological profile of the various epileptogenic lesions in epilepsy surgery patients was analyzed. Based on this profile, a predictive model was developed. This model offers excellent potential to identify the nature of the underlying lesion prior to resection. If validated, this model may be particularly valuable for counseling patients, as depending on the lesion type, different outcomes are achieved after epilepsy surgery.

KEYWORDS

connectivity, epileptogenicity, focal cortical dysplasia, gliosis, high-frequency oscillations, hippocampal sclerosis, spikes

1 | INTRODUCTION

Modern neuroimaging techniques have dramatically improved the identification of potentially epileptogenic lesions. For several reasons, however, a significant degree of uncertainty persists, and in many patients, lesions cannot be well identified *in vivo* or their role in the epileptogenic process remains uncertain. Not all visible lesions are epileptogenic and hence responsible for seizure generation.¹ Also, contrary to well-identified brain tumors, not all epileptogenic lesions can be identified on standard magnetic resonance imaging (MRI) scans.² Finally, the histopathological nature of a given lesion based “only” on its MRI appearance is often inconclusive (Wang et al.).^{1,3}

Typically, the histopathological specimens of drug-resistant epileptic patients are, besides tumors, hippocampal sclerosis (HS), focal cortical dysplasia (FCD), nonspecific gliosis (NG), or histologically normal tissue (NT).⁴ Histopathological examination is the only way to reliably determine the lesion type (HS vs. FCD vs. NG vs. NT), and the long-term seizure freedom after resection is necessary to ascertain its epileptogenicity.

We designed this study to analyze electrophysiological biomarkers characterizing different types of pathology using invasive electroencephalography (EEG; stereo-EEG [SEEG]) in drug-resistant epileptic patients. We selected the following biomarkers: (1) interictal spikes, (2) high-frequency oscillations (HFOs), and (3) functional connectivity measures.

Spikes are traditionally used for epilepsy diagnostics and can be used as a marker of tissue epileptogenicity (Staley &

Key Points

- The highest rates of spikes were found in HS compared to FCD and NG/NT
- Duration and amplitude of spikes were higher in NG/NT than HS and FCD
- Ripples showed higher relative rates for HS and NG/NT than FCD
- Duration of ripples was longer for NG/NT than FCD
- HFO amplitude of ripples was higher in HS and NG/NT than FCD; in contrast, the amplitude of fast ripples presented higher values in FCD than NG/NT
- All studied connectivity measures indicated significant differences in the functional connectivity between the individual epileptogenic lesions
- A predictive model of the underlying brain pathology was developed based on all assessed interictal measures

Dudek).⁵ Pathological interictal HFOs were proved to be the markers of several processes within the epileptic brain. They reflect fundamental neuronal disturbances in areas generating spontaneous seizures and localize the epileptogenic region independently of the underlying lesion. They also determine the severity of epileptogenicity and even predict epilepsy development.^{6,7} Despite the extensive research on HFOs and their characteristics, knowledge on

their relationship to the underlying pathological substrates remains scarce. Studies exploring HFOs in different epileptogenic lesions are scarce and reach divergent results. Jacobs et al.⁸ found no specific HFO pattern characteristics studying 12 patients with HS, FCD, or nodular heterotopia. Kerber et al.⁹ compared HFO rates between patients with FCD type I versus type II, and found that HFO rates were significantly higher in FCD type II, suggesting that the activity of HFOs mirrors disease activity. A more extensive study with 37 patients was conducted by Ferrari-Marinho et al. The authors showed a significant difference in ripple and fast ripple rates with respect to the lesion type; higher rates were present in FCD, HS, and nodular heterotopia compared to atrophy, polymicrogyria, and tuberous sclerosis. Focusing on the subtype of FCD patients, the HFO rates differed based on the spatial relation to the MRI pathology. The rates were highest in the borders of MRI-visible dysplastic lesions, followed by the surrounding area, and only rare HFOs were present in the remote cortex. Limitations of this study, however, are the absence of histopathological verification in all patients and inclusion independently of the surgery outcome.¹⁰

Functional connectivity allows exploration of dynamic network processes in the brain tissue (Fingelkurts et al.).¹¹ However, there is no single optimal method for functional connectivity assessment, and differences between the methods employed yield variable results. Functional MRI allows indirect measurement of neuronal activity through blood oxygenation patterns but permits whole-brain connectivity analysis. Studies employing functional MRI reported either decreased interictal connectivity in focal epilepsy patients^{12,13} or increased connectivity in some networks juxtaposed with decreases in others.^{14,15} By contrast, SEEG provides direct neuronal recordings from the human brain, but only from anatomy covered by the electrodes.^{16,17} Studies using intracranial EEG recordings have suggested predominantly increased interictal connectivity involving the epileptogenic zone (EZ) and surrounding structures,^{18–20} with the seizure onset zone (SOZ) functionally isolated from overlaying healthy tissue.^{21,22} In FCD type II, increased phase-amplitude coupling was reported in areas containing dysmorphic neurons.²³ Otherwise, there is, to our knowledge, no available information about differences in functional connectivity dependent on the underlying pathology.

In the present article, we aimed to study spikes and HFOs, including their characteristics and functional connectivity on SEEG in patients with various pathological substrates. We hypothesized that epilepsy with a specific underlying pathology (HS, FCD, NG, or NT) would diverge in electrophysiological biomarkers and subsequently in neuronal network organization as well as its epileptogenicity potential.

2 | MATERIALS AND METHODS

We retrospectively reviewed the data of drug-resistant epileptic patients who underwent SEEG and subsequent surgery at the Montreal Neurological Institute and Hospital (MNI) and St. Anne's University Hospital (SAUH). We included patients with specific histopathological findings, namely FCD, HS, NG, and NT, that were postoperatively categorized as seizure-free (Engel I at Year 1 after surgery). We analyzed a resting-state SEEG recording for each patient, identifying the electrophysiological differences in spikes, HFOs, and functional connectivity measures between individual histopathological groups. Ethical committee boards approved the study at both institutions.

2.1 | Subject selection

We reviewed all patients who underwent brain surgery after SEEG investigation for drug-resistant epilepsy at MNI and SAUH. The inclusion criteria for this study were as follows: (1) surgery outcome classified as Engel I at Year 1 after the surgery; (2) availability of seizure-free SEEG recording in resting state (wakefulness with closed eyes) for a given patient; (3) availability of the precise position of individual SEEG electrodes and contacts; and (4) histopathological examination of the resected tissue with the presence of FCD, HS, NG or NT. We excluded patients with previous brain surgery, other histopathological results comprising fewer than five cases in the whole dataset, bitemporal epilepsy based on SEEG results, or unfavorable postoperative result to ascertain genuine epileptogenicity of the resected tissue.

Histopathological evaluation was made by two experienced neuropathologists according to International League Against Epilepsy classification criteria for HS²⁴ and FCD.²⁵ The postsurgical outcome was classified according to Engel et al.²⁶ by a board-certified clinical epileptologist (B.F. or M.P.).

2.2 | Recordings selection and processing

Depth electrodes were implanted using the stereotactic navigation system according to the anatomoelectroclinical findings tailored for each patient. Homemade and later DIXI electrodes were employed at MNI, and ALCIS electrodes were used at SAUH (for electrode specification, see Data S2). The position of electrodes was coregistered with magnetic resonance and computed tomographic images. Resected contacts were determined from postresection MRI. Channels that revealed the first ictal activity leading to an apparent seizure in the ictal SEEG independent of the fast activity content were labeled as SOZ contacts by

board-certified neurophysiologists (I.D., B.F., F.D., R.P., and M.P.). We evaluated only contacts that overlapped with resected tissue and SOZ. The minimum was two pairs of contacts per patient.

All SEEG data were recorded during resting wakefulness with eyes closed in standardized conditions. In the case of MNI, controlled periods of resting wakefulness with closed eyes were selected from routine EEG recordings acquired using the Harmonie long-term monitoring system (Stellate) with a sampling frequency of 1000 Hz with the low pass filter of 600 Hz. In the case of SAUH patients, 30 min of continuous wide-bandwidth (recorded with sampling rate of 25000 Hz and downsampled to 5000 Hz with a 2000-Hz frequency band) recordings were analyzed. At both institutions, a referential montage was used for acquisition with an epidural electrode fixed in the bone, far from the epileptic field as reference.

All recordings were manually checked for the presence of seizures or significant artifacts by two board-certified neurophysiologists (I.D. and M.P.). Recordings from both institutions were used for detection and computation in the ripple band, whereas for the fast ripple band, we used only SAUH recordings due to the sampling frequency.

2.3 | Detection of spikes and HFOs

Spikes and HFOs were identified using established detectors.^{27,28} Spikes were computed within the 1–80-Hz frequency band. HFOs were subdivided into ripples (80–250 Hz) and fast ripples (250–500 Hz). Both spikes and HFOs were evaluated for their rates, amplitudes, and duration.

2.4 | Computation of connectivity measures

Functional connectivity is a model of statistical dependencies of neurophysiological time series. Relative entropy (REN), for instance, evaluates the randomness and spectral richness between two time series; in other words, it is a measure of how entropy of one signal diverges from a second, expected one. The value of REN varies in interval $<0, +\infty>$. $REN=0$ indicates the equality of statistical distributions of two signals, whereas $REN>0$ indicates that the two signals are carrying different information. In other words, high REN values indicate low functional connectivity and vice versa.

Statistically significant differences in REN values were reported in the EZ compared to non-EZ structures; thus, it is perceived as a novel biomarker of the EZ.²⁹ Established functional connectivity measures—apart from REN, linear

correlation, cross-correlation, and phase consistency—were computed for adjacent pairs of referential channels contained in the resected tissue and SOZ for frequencies within the spike, ripple, and fast ripple bands.

2.5 | Statistical analyses and predictive model

All studied features were normalized by dividing individual channel values by the sum of the channel values within each patient and frequency band. The differences between pathologies were evaluated with a Wilcoxon signed-rank test with Bonferroni corrections and Cliff delta as effect size measure.

Based on the studied features, we constructed a machine learning model predicting the underlying pathology. Because of the small number of features, no feature selection was performed. We first investigated different machine learning algorithms (support vector machine, logistic regression, decision tree) and their hyperparameters by iteratively evaluating their performance using the F-score as the performance metric. The best model and its hyperparameters were used to create a generalized model. Besides the F-score, we additionally computed the model accuracy. We evaluated both the prediction performance for a single channel and the pathology as a whole (subject pathology; reaching 50% prediction success over all evaluated channels).

We used both leave-one-channel-out (LOCHO; across all patients) and leave-one-patient-out (LOPO) approaches to evaluate each iteration, where one channel/patient was withheld for validation, and the rest of the channels/patients were used for the training of the model. Due to low sampling frequency in the MNI dataset, we constructed models (both LOPO and LOCHO) using only the ripple band for the whole dataset. We additionally constructed models including fast ripple band only for the SAUH dataset.

3 | RESULTS

3.1 | Patient characteristics

3.1.1 | MNI patients

Seizure-free outcomes defined as Engel I were obtained in 24 patients after resective surgery between 2005 and 2019. Twelve patients were excluded for the following reasons: follow-up was lost in one, unavailability of histopathology in two, previous surgery in one, and unavailability of the position of electrodes or resting-state SEEG in eight

patients. A total of 12 patients were analyzed: 10 with FCD (104 channels), one with HS (six channels), and one with NG/NT (six channels).

3.1.2 | SAUH patients

Resective brain surgery for epilepsy resulted in Engel I postoperative outcome in 24 patients between 2012 and 2019. Three patients were excluded (multiple surgeries in one patient, and two patients had different types of pathology as defined in the inclusion criteria [arteriovenous malformation or nodular heterotopia]). In total, 21 patients were analyzed: five with FCD (17 channels), seven with HS (25 channels), and nine with NG/NT (48 channels).

The cohort included 33 subjects (19 women) with a median age at surgery of 29 years (minimum = 10 years, maximum = 57 years) and a median epilepsy duration of 16 years. Three patients had a positive family history of epilepsy, two patients had febrile seizures, two had a history of encephalitis/meningitis, and two had a history of brain trauma.

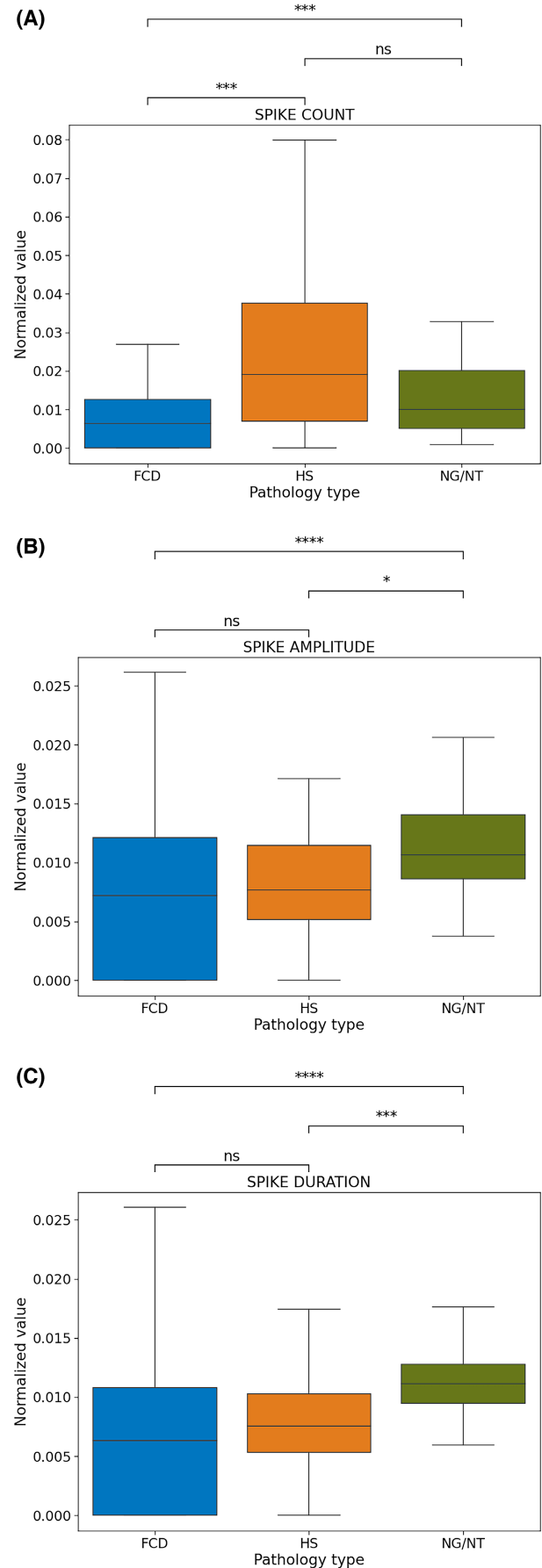
There was histopathologically proven FCD in 15 (type I in one, type II in 13, and type III [FCD associated with ganglioglioma] in one), HS in eight, NG in four, and NT in six patients. The NG/NT group consisted of four hippocampal resections, five cortical, and one combination of both. Considering the sizes of the NG and NT groups, we grouped them for further analysis (NG/NT group).

Considering the MRI results altogether, 20 of 33 patients had an inconclusive presurgical MRI.

3.2 | Differences in spike characteristics between HS, FCD, and NT/NG

The highest spike rates were present in HS, followed by NG/NT and FCD (see Figure 1). The differences in spike count were significant between patients with HS and FCD ($p < .001$, $d = -.472$) and between HS and NG/NT ($p < .0001$, $d = .208$). No differences were found between FCD and NG/NT. Both the duration and amplitude of the spikes were highest in the case of NG/NT, followed by HS and FCD;

FIGURE 1 Differences in interictal spike characteristics, namely count (A), amplitude (B), and duration (C), between focal cortical dysplasia (FCD), hippocampal sclerosis (HS) and nonspecific gliosis/normal tissue (NG/NT). Boxplots report average values per individual channel. The box shows the quartiles of the dataset, and the whiskers extend to show the rest of the distribution. Outliers are not visualized. * $p = .05$, *** $p = .001$, **** $p = .0001$. ns, not significant.



however, only differences between NG/NT and HS (duration $p < .0001$, $d = -.471$; amplitude $p < .001$, $d = -.372$) and between NG/NT and FCD (duration $p < .001$, $d = -.503$; amplitude $p < .05$, $d = -.396$) reached statistical significance.

3.3 | Differences in HFO characteristics between HS, FCD, and NT/NG

Both NG/NT ($p < .0001$, $d = -.430$) and HS ($p < .01$, $d = -.404$) showed higher ripple rates compared to FCD (see Figure 2). There were no significant differences between HS and NG/NT.

Considering HFO duration in the ripple band, only the difference between FCD and NG/NT was significant ($p < .01$, $d = -.329$), in favor of NG/NT. The highest amplitude of ripples was present in NG/NT, followed by HS and FCD. Only the differences between NG/NT versus FCD ($p < .0001$, $d = -.4617$) and HS versus FCD ($p < .05$, $d = -.290$) proved to be significant.

Higher amplitude for FCD versus NG/NT ($p < .05$, $d = .404$) was found in the limited sample available for fast ripple band analysis. Considering the HFO rate and duration, there were no significant differences between the studied groups.

3.4 | Connectivity measures

We performed four connectivity measures. In the spike band, both the cross-correlation ($p < .05$, $d = .2910$) and linear correlation ($p < .05$, $d = .2939$) showed higher connectivity in FCD versus HS (see Figure 3). Differences in the REN of phase consistency in spike band failed to reach statistical significance levels.

Within the ripple frequency band employing REN were found higher values (signaling lower functional connectivity) in HS compared to FCD ($p < .01$, $d = -.346$). Phase consistency showed higher values with NG/NT compared to HS ($p < .05$, $d = -.354$; see Figure 3). Differences between NG/NT and FCD did not reach statistical significance. Linear correlation and cross-correlation did not show statistically significant differences between the three groups within the ripple band.

The limited patient sample available for the fast ripple analyses showed both REN and phase consistency results

corresponding to ripples: REN in HS versus FCD ($p < .05$, $d = -.473$) and phase consistency with higher values in NG/NT compared to HS ($p < .05$, $d = -.398$). Additionally, higher REN for HS versus NG/NT was present in the fast ripple band ($p < .001$, $d = .545$).

3.5 | Predictive model

The best performing algorithm was a support vector machine with rbf kernel and $C = 1$ with the LOCHO approach including both the ripple and fast ripple ranges. Using only the ripple band, the model achieved 84.0% accuracy and 82.1% F-score for channel prediction and 76.7% accuracy and 77.6% F-score for the prediction of subject pathology. Using the LOPO approach, the results for both datasets showed lower performance, with 42.6% accuracy and 35.0% F-score for channel prediction and 40.4% accuracy and 40.4% F-score for the prediction of subject pathology. The results are summarized in Table 1. The top three features driving the model were phase consistency, REN (fast ripple band), and spike rate.

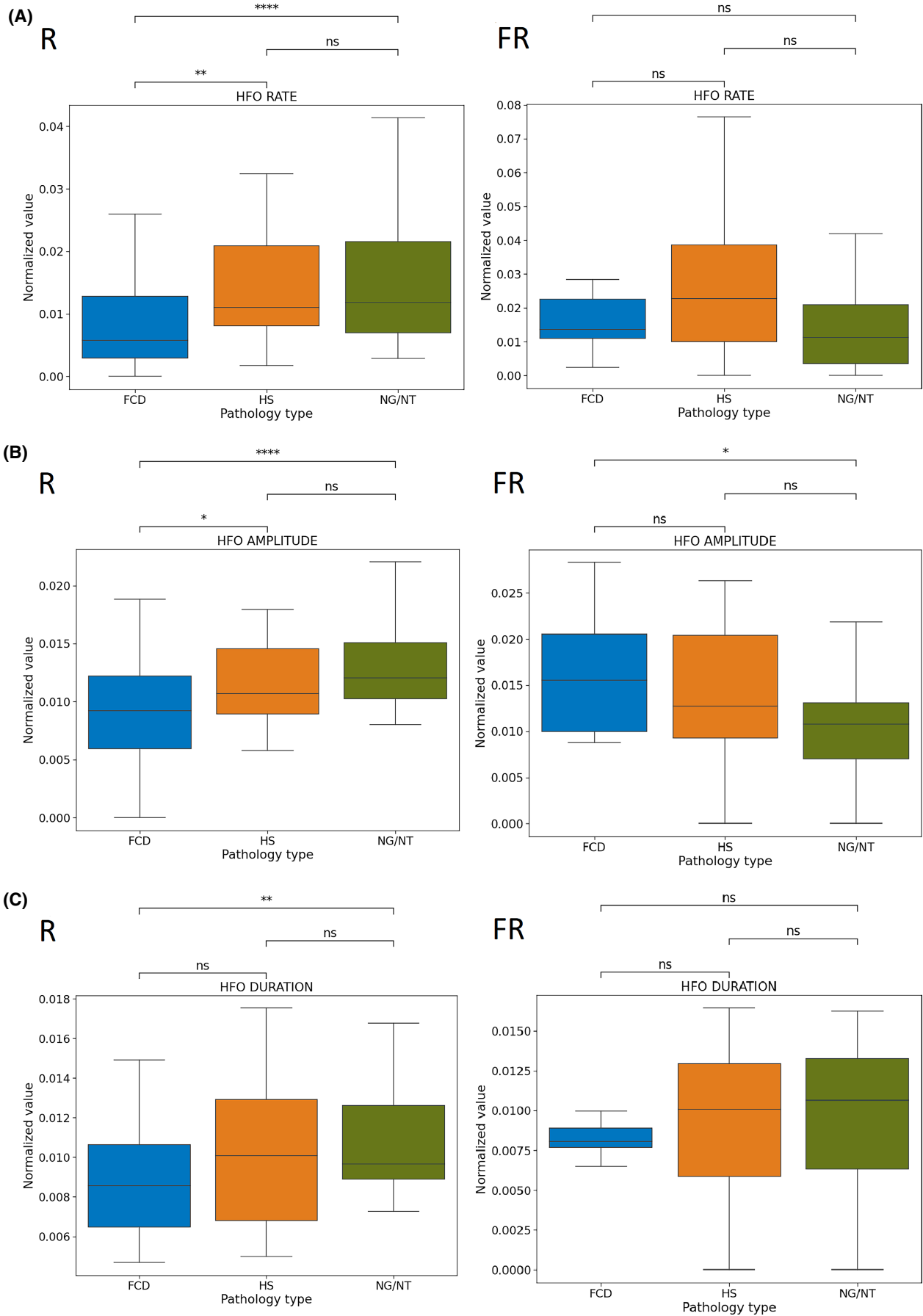
In the group of 20 patients with inconclusive MRI results was the LOCHO model prediction correct in 16 patients and the LOPO model in 12 patients (for details, see Supporting Information 3).

4 | DISCUSSION

The precise nature of epileptogenic lesions is often demonstrated only in vitro and when the surgical specimen is available. In this study, we propose an original approach to improve the in vivo characterization of those lesions. We analyzed spike and HFO characteristics and connectivity measures in SEEG studies of selected patients with intractable focal epilepsy and developed a predictive model to determine a neurophysiological signature of the underlying epileptogenic lesion. We compared three frequent epileptogenic surgical lesions, HS, FCD, and NG/NT, and their SEEG interictal electrophysiological characteristics, and found for each group a characteristic fingerprint.

Spikes were found in all lesion types in all patients. This finding indicates that spikes are reliable markers of tissue epileptogenicity. Regarding spike characteristics, spike rates were the highest in HS compared to other

FIGURE 2 Differences in high-frequency oscillation (HFO) rate (A), amplitude (B), and duration (C) between focal cortical dysplasia (FCD), hippocampal sclerosis (HS), and nonspecific gliosis/normal tissue (NG/NT). The ripple band (R) was evaluated in 33 patients, the fast ripple band (FR) in 21 patients. Boxplots report average values per individual channel (for effect sizes, see Data S1). The box shows the quartiles of the dataset, and the whiskers extend to show the rest of the distribution. Outliers are not visualized. * $p = .05$, ** $p = .01$, *** $p = .0001$. ns, not significant.



pathological groups. This finding is not surprising and corresponds with several human and animal studies.^{30–32}

Rather surprising and unprecedented, however, was that the FCD group showed lower spike rates than NG/NT. This could be influenced by the timing of the sampling (i.e., daytime, at rest), because the highest spiking rates in FCD and in particular FCD type II were shown in non-rapid eye movement sleep.^{33,34} Also, the discovery that the duration and amplitude of spikes are higher in NG/NT than HS and FCD was not reported previously and adds another piece of evidence to the specific fingerprint of studied pathologies.

The other evaluated marker was HFOs. HFOs, both ripples and fast ripples, were found in all pathologies, supporting the high level of epileptogenicity of all studied substrates. The highest rates of HFO ripples were found in HS, in accordance with the results of other studies.^{8,35}

The surprising finding of our work is that ripple rates were found to be higher in NG/NT compared to FCD. To some extent, this could be influenced by the hippocampal origin of the resected tissue in part of the NG/NT group. Another explanation could be that the representative part of the pathology was removed by suctioning during the resection process. Amplitude and duration of ripples also presented higher values in NG/NT (together with HS) than FCD. Interestingly, fast ripples indicated opposing results, with FCD having a higher amplitude than NG/NT. Because HFOs were already shown to mirror the disease activity of the brain tissue and even play a part in seizure genesis,^{9,35,36} they are currently the most accurate markers of tissue epileptogenicity. In this context, the most pronounced epileptogenicity seems to reside in HS and NG/NT. Finding that FCD presents with lower amplitude than NG/NT in ripples and higher amplitude in fast ripples is novel and potentially determines specific fingerprints of these pathologies.

All studied connectivity measures indicated significant differences in the functional connectivity between the individual epileptogenic lesions.

In agreement, the cross-correlation and linear correlation within the spike band and REN with phase consistency in the ripple and fast ripple bands indicated lower functional connectivity in HS compared to FCD or NG/NT. Differences between FCD and NG/NT showed only an insignificant trend, with slightly higher values in FCD. Chronic alterations of the functional organization were

revealed in focal epilepsy both at the level of the lesional tissue³⁷ and in the large-scale corticosubcortical networks. The most striking example of these alterations is FCD,³⁸ with inefficient global and excessive local connectivity,³⁹ corresponding to presented results.

Aberrant connectivity within the epileptogenic lesion supposedly stems from the formation of local epileptic networks.⁷² Studies on focal epilepsies demonstrated enhanced connectivity in the EZ and the presence of highly interconnected nodes presumably playing a crucial role in the onset and propagation of ictal activity.^{40,41} Because gliosis was previously shown to comprise a more extensive area than lesion visible on MRI,^{42,43} supposedly more interconnected nodes are involved, raising the level of connectivity compared to the relatively small area in mesiotemporal sclerosis.

4.1 | Electrophysiological profile

The novelty of this study is a newly established predictive model showing a potential for prediction of underlying pathology based solely on the interictal electrophysiological parameters. Such a model has not been developed yet to our knowledge. This model offers potential to discern the nature of the underlying pathology prior to resective surgery as demonstrated by the correct prediction of the majority of patients in our cohort with inconclusive pre-surgical MRI. Further testing on bigger sample sizes is, however, needed.

Further information in the form of electrophysiological and connectivity profiles pointing to a specific lesion type may grow in importance when delineating the EZ. Temporal lobe epilepsy with unilateral mesial temporal sclerosis has an EZ frequently limited to the mesiotemporal area, and its resection results in seizure cessation.⁴⁴ In the case of FCD type I and III or cortical gliosis, the situation seems more complicated; the EZ often comprises a more extensive area than the lesion visible on the imaging techniques. The outcome of the surgical resection consequently does not reach excellent results.^{42,43}

The question remains whether the mechanism underlying seizure generation and epileptogenicity differs depending on the lesion type. Perucca and his colleagues showed that biologically distinct epileptogenic lesions share intracranial electroencephalographic seizure-onset

FIGURE 3 Boxplot showing connectivity measure results—cross-correlation within spike band (A), linear correlation within spike band (B), relative entropy (C), and phase consistency (D)—for each lesion type in spike, ripple (R), or fast ripple (FR) bands: focal cortical dysplasia (FCD), hippocampal sclerosis (HS), and nonspecific gliosis/normal tissue (NG/NT). The spike and ripple band were evaluated in 33 patients, and the fast ripple band in 21 patients. The box shows the quartiles of the dataset, and the whiskers extend to show the rest of the distribution. Outliers are not visualized. * $p = .05$, ** $p = .01$, *** $p = .001$, **** $p = .0001$. ns, not significant.

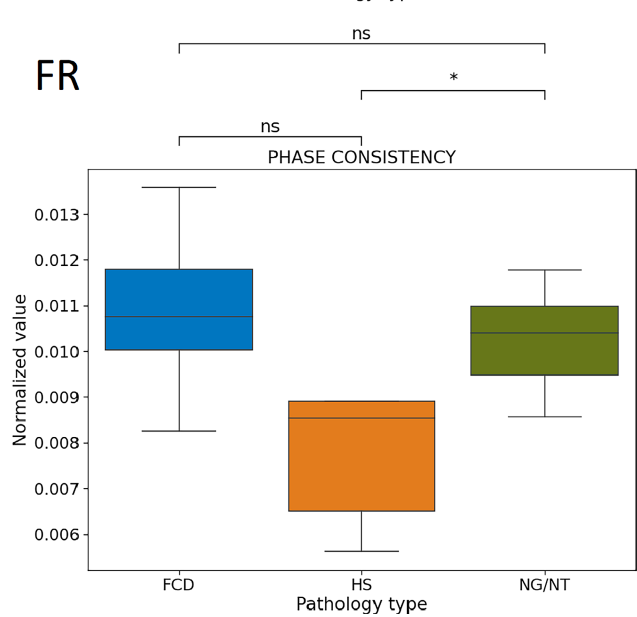
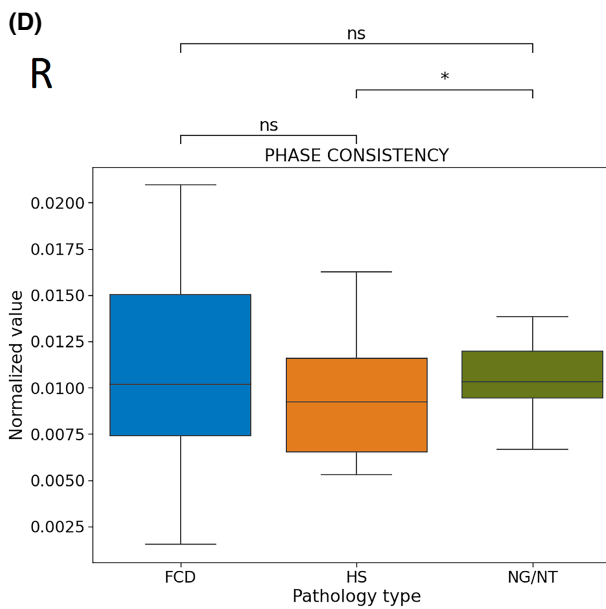
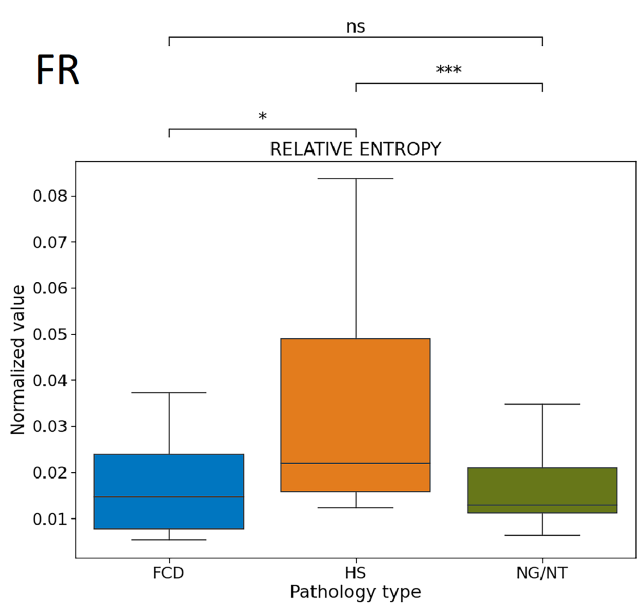
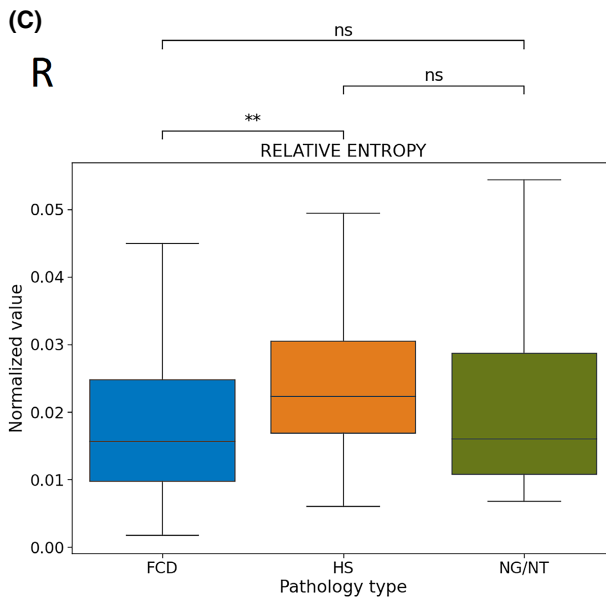
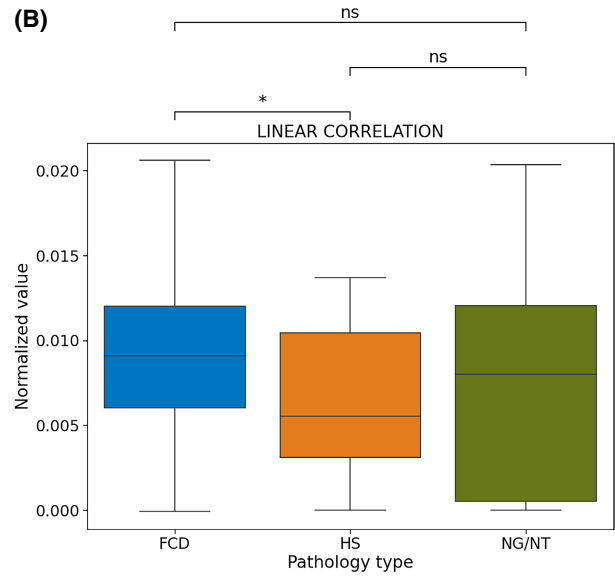
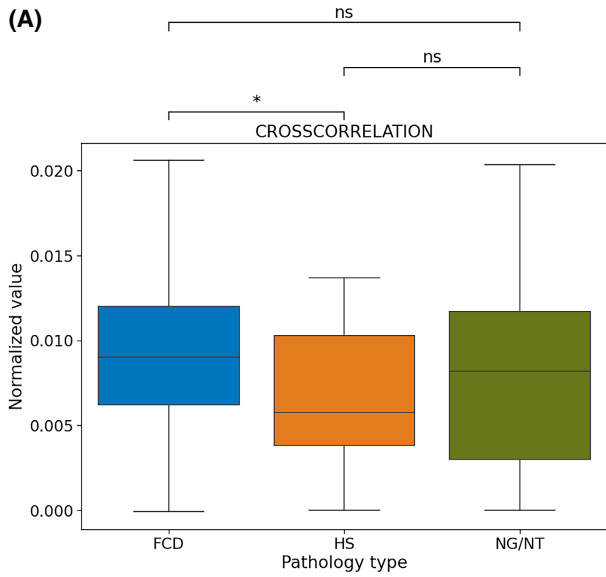


TABLE 1 Characteristics of the established predictive models.

Model	Institution	Channel prediction accuracy	Channel prediction F-score	Subject pathology prediction accuracy	Subject pathology prediction accuracy F-score
LOCHO including FR band	SAUH	.8783	.871	.8308	.8581
LOPO including FR band	SAUH	.3739	.3528	.3633	.403
LOCHO without FR band	MNI + SAUH	.8398	.8202	.7672	.7764
LOPO without FR band	MNI + SAUH	.6494	.6286	.5909	.5909

Abbreviations: FR, fast ripple; LOCHO, leave one channel out; LOPO, leave one patient out; MNI, Montreal Neurological Institute and Hospital; SAUH, St. Anne's University Hospital.

patterns and suggested that different pathological substrates can affect similar networks or mechanisms underlying seizure generation.⁴⁵

On the other hand, the finding that studied epileptogenic substrates differed substantially in their electrophysiological profiles advocate for different underlying mechanisms such as excitotoxic damage, malfunctioning of dysmorphic neurons or glial cells, or network disruption due to the cytoarchitectonic aberrations.

It is important that when a histopathological report is deemed normal, it does not actually include abnormalities on a subcellular level.^{46,47} If that is the case, it may include a potentially important node of a broader malfunctioning network. Its elimination may result in seizure freedom, which supposedly was the mechanism behind seizure freedom in the patients from the NT group.

4.2 | Limitations and future directions

Some limitations of this study require attention. The volume of recording of each SEEG electrode contact is necessarily limited to the surrounding tissue. Because the extent of the lesion and consequently its resection is limited in some patients, the number of evaluated contacts differs across the whole cohort.

A major limitation of the predictive model is the inclusion of only one patient with HS and NT/NG pathologies in the MNI dataset. This might artificially raise the performance of the model trained on the whole dataset. We have addressed this by computing separately parameters for channel prediction and subject pathology prediction (see Table 1 for details). Even though each electrode contact is placed in a different anatomical location in an individual patient, the LOCHO approach for pathology prediction can potentially show falsely higher performance, because the training of the model is performed

on the channels from a patient from whom the testing channel is selected.

Also, for technical reasons (sampling frequency), fast ripple frequency band analyses were limited to a small number of patients. Further studies are needed to extend the spectrum of studied pathological substrates such as nodular heterotopia, tuberous sclerosis, or polymicrogyria. A bigger sample size would allow for the differentiation and comparison of individual FCD subtypes.

Future analyses focusing on the connectivity between the pathology and other brain regions are needed.

5 | CONCLUSIONS

This study analyzed electrophysiological profiles of common epileptogenic lesions in interictal SEEG recordings from epileptic patients treated surgically with excellent results. Statistically significant differences were found between the individual pathologies in the HFO rates, spikes, and their characteristics, with the highest values in the case of HS, and functional connectivity measures with the lowest values in the case of HS.

A predictive model of the nature of the lesion based on an electrophysiological profile was established, which might be particularly valuable in the surgical treatment of epilepsy. If validated, it might be a very useful tool for counseling of patients, as depending on the lesion type different outcomes are achieved after epilepsy surgery. Our work demonstrated different levels of epileptogenicity of individual pathologies and suggests different epileptogenic mechanisms in individual pathological tissues.

AUTHOR CONTRIBUTIONS

All authors had full access to all the data in the study and take responsibility for the integrity of the data and the accuracy of the data analysis. Conceptualization: Eva Zatloukalova,

Barbora Sklenarova, Milan Brazdil. Methodology: Eva Zatloukalova, Barbora Sklenarova, Jan Cimbalnik. Investigation: Jan Cimbalnik, Petr Klimes, Birgit Frauscher, Jean Gotman, Marketa Hermanova, Michal Hendrych, Martin Pail, Irena Dolezalova, Raluca Pana, Jeffrey Hall, François Dubeau, Jitka Kocvarova. Formal analysis: Jan Cimbalnik, Petr Klimes. Resources: Milan Brazdil, Birgit Frauscher. Writing—original draft: Eva Zatloukalova, Barbora Sklenarova, Irena Dolezalova. Writing—review & editing: Eva Zatloukalova, Barbora Sklenarova, Irena Dolezalova, Milan Brazdil, Birgit Frauscher. Visualization: Jan Cimbalnik, Petr Klimes. Supervision: Milan Brazdil. Project administration: Eva Zatloukalova, Barbora Sklenarova. Funding acquisition: Milan Brazdil, Birgit Frauscher.

ACKNOWLEDGMENTS

MNI: This work was funded by a project grant from the Canadian Institutes of Health Research (PJT-175056) and a generous donation by the Hewitt Foundation. B.F. is supported by a salary award (Chercheur-boursier clinicien Senior) of the Fonds de Recherche du Québec—Santé 2021-2025. SAUH: AZV NU22-08-00278, AZV NU22-04-00366, GACR 22-28784S. Supported by project LX22NPO5107 (MEYS), financed by the European Union—Next Generation EU.

CONFLICT OF INTEREST STATEMENT

None of the authors has any conflict of interest to disclose.

ORCID

Barbora Sklenarova  <https://orcid.org/0000-0002-7265-9416>

Eva Zatloukalova  <https://orcid.org/0000-0003-4364-532X>

Jan Cimbalnik  <https://orcid.org/0000-0001-6670-6717>

Petr Klimes  <https://orcid.org/0000-0002-0232-9518>

Irena Dolezalova  <https://orcid.org/0000-0002-3166-4817>

Martin Pail  <https://orcid.org/0000-0003-2059-4822>

Jitka Kocvarova  <https://orcid.org/0000-0001-9139-1091>

Michal Hendrych  <https://orcid.org/0000-0002-1024-7408>

Marketa Hermanova  <https://orcid.org/0000-0002-3889-0905>

Jean Gotman  <https://orcid.org/0000-0002-9796-5946>

Raluca Pana  <https://orcid.org/0000-0003-2590-1983>

Birgit Frauscher  <https://orcid.org/0000-0001-6064-1529>

Milan Brazdil  <https://orcid.org/0000-0001-7979-2343>

REFERENCES

- Cendes F, Theodore WH, Brinkmann BH, Sulc V, Cascino GD. Neuroimaging of epilepsy. *Handb Clin Neurol*. 2016;136:985–1014.

- von Oertzen J, von Oertzen J. Standard magnetic resonance imaging is inadequate for patients with refractory focal epilepsy. *J Neurol Neurosurg Psychiatry*. 2002;73:643–7. <https://doi.org/10.1136/jnnp.73.6.643>
- Wang ZI, Alexopoulos AV, Jones SE, Jaisani Z, Najm IM, Prayson RA. The pathology of magnetic-resonance-imaging-negative epilepsy. *Mod Pathol*. 2013;26(8):1051–8.
- Blumcke I, Spreafico R, Haaker G, Coras R, Kobow K, Bien CG, et al. Histopathological findings in brain tissue obtained during epilepsy surgery. *N Engl J Med*. 2017;377(17):1648–56.
- Staley KJ, Dudek FE. Interictal spikes and epileptogenesis. *Epilepsy Curr*. 2006;6(6):199–202.
- Jacobs J, Zijlmans M. HFO to measure seizure propensity and improve prognostication in patients with epilepsy. *Epilepsy Curr*. 2020;20(6):338–47.
- Staba RJ, Bragin A. High-frequency oscillations and other electrophysiological biomarkers of epilepsy: underlying mechanisms. *Biomark Med*. 2011;5:545–56. <https://doi.org/10.2217/bmm.11.72>
- Jacobs J, LeVan P, Châtillon C-É, Olivier A, Dubeau F, Gotman J. High frequency oscillations in intracranial EEGs mark epileptogenicity rather than lesion type. *Brain*. 2009;132:1022–37. <https://doi.org/10.1093/brain/awn351>
- Kerber K, LeVan P, Dümpelmann M, Fauser S, Korinthenberg R, Schulze-Bonhage A, et al. High frequency oscillations mirror disease activity in patients with focal cortical dysplasia. *Epilepsia*. 2013;54:1428–36. <https://doi.org/10.1111/epi.12262>
- Ferrari-Marinho T, Perucca P, Mok K, Olivier A, Hall J, Dubeau F, et al. Pathologic substrates of focal epilepsy influence the generation of high-frequency oscillations. *Epilepsia*. 2015;56:592–8. <https://doi.org/10.1111/epi.12940>
- Fingelkurts AA, Fingelkurts AA, Kähkönen S. Functional connectivity in the brain—is it an elusive concept? *Neurosci Biobehav Rev*. 2005;28(8):827–36.
- Luo C, Qiu C, Guo Z, Fang J, Qifu Li X, Lei YX, et al. Disrupted functional brain connectivity in partial epilepsy: a resting-state fMRI study. *PLoS One*. 2011;7(1):e28196.
- Voets NL, Beckmann CF, Cole DM, Hong S, Bernasconi A, Bernasconi N. Structural substrates for resting network disruption in temporal lobe epilepsy. *Brain*. 2012;135(Pt 8):2350–7.
- Liao W, Zhang Z, Pan Z, Mantini D, Ding J, Duan X, et al. Altered functional connectivity and small-world in mesial temporal lobe epilepsy. *PLoS One*. 2010;5(1):e8525.
- Luo C, An D, Yao D, Gotman J. Patient-specific connectivity pattern of epileptic network in frontal lobe epilepsy. *NeuroImage Clin*. 2014;4(April):668–75.
- Hyder F, Rothman DL. Quantitative fMRI and oxidative Neuroenergetics. *Neuroimage*. 2012;62(2):985–94.
- Yuan J, Chen Y, Hirsch E. Intracranial electrodes in the presurgical evaluation of epilepsy. *Neurol Sci*. 2012;33(4):723–9.
- Bartolomei F, Bettus G, Stam CJ, Guye M. Interictal network properties in mesial temporal lobe epilepsy: a graph theoretical study from intracerebral recordings. *Clin Neurophysiol*. 2013;124(12):2345–53.
- Bettus G, Wendling F, Guye M, Valton L, Régis J, Chauvel P, et al. Enhanced EEG functional connectivity in mesial temporal lobe epilepsy. *Epilepsy Res*. 2008;81(1):58–68.
- Zaveri HP, Pincus SM, Goncharova II, Duckrow RB, Spencer DD, Spencer SS. Localization-related epilepsy exhibits significant

- connectivity away from the seizure-onset area. *Neuroreport*. 2009;20(9):891–5.
21. Klimes P, Duque JJ, Brinkmann B, Van Gompel J, Stead M, St EK, et al. The functional organization of Human epileptic hippocampus. *J Neurophysiol*. 2016;115(6):3140–5.
 22. Warren CP, Sanqing H, Stead M, Brinkmann BH, Bower MR, Worrell GA. Synchrony in Normal and focal epileptic brain: the seizure onset zone is functionally disconnected. *J Neurophysiol*. 2010;104:3530–9. <https://doi.org/10.1152/jn.00368.2010>
 23. Rampf S, Rössler K, Hamer H, Illek M, Buchfelder M, Doerfler A, et al. Dymorphic neurons as cellular source for phase-amplitude coupling in focal cortical dysplasia type II. *Clin Neurophysiol*. 2021;132(3):782–92.
 24. Blümcke I, Thom M, Aronica E, Armstrong DD, Bartolomei F, Bernasconi A, et al. International consensus classification of hippocampal sclerosis in temporal lobe epilepsy: a task force report from the ILAE commission on diagnostic methods. *Epilepsia*. 2013;54(7):1315–29.
 25. Blümcke I, Thom M, Aronica E, Armstrong DD, Vinters HV, Palmini A, et al. The clinicopathologic spectrum of focal cortical dysplasias: a consensus classification proposed by an ad hoc task force of the ILAE diagnostic methods commission. *Epilepsia*. 2011;52(1):158–74.
 26. Engel J. (Ed). *Surgical treatment of the epilepsies*, 2nd edition. New York: Raven Press;1993. p. 786.
 27. Barkmeier DT, Shah AK, Flanagan D, Atkinson MD, Agarwal R, Fuerst DR, et al. High inter-reviewer variability of spike detection on intracranial EEG addressed by an automated multi-channel algorithm. *Clin Neurophysiol*. 2012;123(6):1088–95.
 28. Cimbalknik J, Hewitt A, Worrell G, Stead M. The CS algorithm: a novel method for high frequency oscillation detection in EEG. *J Neurosci Methods*. 2018;293:6–16.
 29. Cimbalknik J, Klimes P, Sladky V, Nejedly P, Jurak P, Pail M, et al. Multi-feature localization of epileptic foci from Interictal, intracranial EEG. *Clin Neurophysiol*. 2019;130:1945–53. <https://doi.org/10.1016/j.clinph.2019.07.024>
 30. Baulac M. MTLTLE with hippocampal sclerosis in adult as a syndrome. *Rev Neurol*. 2015;171(3):259–66.
 31. Mohamed A, Wyllie E, Ruggieri P, Kotagal P, Babb T, Hilbig A, et al. Temporal lobe epilepsy due to hippocampal sclerosis in pediatric candidates for epilepsy surgery. *Neurology*. 2001;56(12):1643–9.
 32. Riban V, Bouillieret V, Pham-Lê BT, Fritschy J-M, Marescaux C, Depaulis A. Evolution of hippocampal epileptic activity during the development of hippocampal sclerosis in a mouse model of temporal lobe epilepsy. *Neuroscience*. 2002;112(1):101–11.
 33. Menezes Cordeiro I, von Ellenrieder N, Zazubovits N, Dubeau F, Gotman J, Frauscher B. Sleep influences the intracerebral EEG pattern of focal cortical dysplasia. *Epilepsy Res*. 2015;113:132–9.
 34. Tassi L, Garbelli R, Colombo N, Brammerio M, Russo GL, Mai R, et al. Electroclinical, MRI and surgical outcomes in 100 epileptic patients with type II FCD. *Epileptic Disord*. 2012;14(3):257–66. <https://doi.org/10.1684/epd.2012.0525>
 35. Jacobs J, LeVan P, Chander R, Hall J, Dubeau F, Gotman J. Interictal high-frequency oscillations (80–500 Hz) are an indicator of seizure onset areas independent of spikes in the human epileptic brain. *Epilepsia*. 2008;49(11):1893–907.
 36. Zijlmans M, Jacobs J, Zelmann R, Dubeau F, Gotman J. High-frequency oscillations Mirror disease activity in patients with epilepsy. *Neurology*. 2009;72(11):979–86.
 37. Besseling RMH, Jansen JFA, de Louw AJA, Mariëlle CG, Vlooswijk MC, Hoeberigs AP, et al. Abnormal profiles of local functional connectivity proximal to focal cortical dysplasias. *PLoS One*. 2016;11(11):e0166022.
 38. Liu W, Lin M, Yue Q, Gong Q, Zhou D, Xintong W. Brain functional connectivity patterns in focal cortical dysplasia related epilepsy. *Seizure*. 2021;87(April):1–6.
 39. Hong S-J, Bernhardt BC, Gill RS, Bernasconi N, Bernasconi A. The Spectrum of structural and functional network alterations in malformations of cortical development. *Brain*. 2017;140(8):2133–43.
 40. Morgan RJ, Soltesz I. Nonrandom connectivity of the epileptic dentate gyrus predicts a major role for neuronal hubs in seizures. *Proc Natl Acad Sci US A*. 2008;105(16):6179–84.
 41. Wilke C, Worrell G, He B. Graph analysis of epileptogenic networks in human partial epilepsy. *Epilepsia*. 2011;52(1):84–93.
 42. Kim DW, Lee SK, Chu K, Park KI, Lee SY, Lee CH, et al. Predictors of surgical outcome and pathologic considerations in focal cortical dysplasia. *Neurology*. 2009;72(3):211–6.
 43. Krsek P, Maton B, Jayakar P, Dean P, Korman B, Rey G, et al. Incomplete resection of focal cortical dysplasia is the Main predictor of poor postsurgical outcome. *Neurology*. 2009;72:217–23. <https://doi.org/10.1212/01.wnl.0000334365.22854.d3>
 44. McIntosh AM. Temporal lobectomy: long-term seizure outcome, late recurrence and risks for seizure recurrence. *Brain*. 2004;127:2018–30. <https://doi.org/10.1093/brain/awh221>
 45. Perucca P, Dubeau F, Gotman J. Intracranial electroencephalographic seizure-onset patterns: effect of underlying pathology. *Brain*. 2014;137(Pt 1):183–96.
 46. Deshpande T, Li T, Herde MK, Becker A, Vatter H, Schwarz MK, et al. Subcellular reorganization and altered phosphorylation of the astrocytic gap junction protein connexin43 in human and experimental temporal lobe epilepsy. *Glia*. 2017;65(11):1809–20.
 47. do Canto AM, Donatti A, Geraldis JC, Godoi AB, da Rosa DC, Lopes-Cendes I. Neuroproteomics in Epilepsy: what do we know so far? *Front Mol Neurosci*. 2020;13:604158.

SUPPORTING INFORMATION

Additional supporting information can be found online in the Supporting Information section at the end of this article.

How to cite this article: Sklenarova B, Zatloukalova E, Cimbalknik J, Klimes P, Dolezalova I, Pail M, et al. Interictal high-frequency oscillations, spikes, and connectivity profiles: A fingerprint of epileptogenic brain pathologies. *Epilepsia*. 2023;64:3049–3060. <https://doi.org/10.1111/epi.17749>